ISBN: 978-3-95450-240-0 ISSN: 2673-5539 doi:10.18429/JACoW-RuPAC2021-WEPSC36

SIMULATION OF THE COHERENT RADIATION INTERFEROMETRY FOR THE BEAM TEMPORAL STRUCTURE DIAGNOSTICS

M. Toktaganova*, D. Shkitov†, M. Shevelev, S. Stuchebrov
Tomsk Polytechnic University, Lenina ave. 2a, 634050 Tomsk, Russia

Abstract

We consider a mathematical model and computer simulation results describing the interferometry of both diffraction and transition radiation to develop an electron bunch train structure diagnostic method. The results of the autocorrelation function simulation indicate a possibility of diagnosing the bunch number in the train as well as spacing between them in case of using narrowband or broadband detectors. The suggested method will allow rejecting spectrum reconstruction in favor of extracting information directly from the autocorrelation function.

INTRODUCTION

Nowadays, free electron lasers and new facilities that are capable of generating sequences of short electron bunches with a high (THz) repetition rate have widely developed [1]. The existing diagnostic methods for such sequences have limitations or are not applicable. Therefore, it is important to develop new approaches to diagnose the temporal structure of such sequences (trains) in modern accelerators. In this report, we describe a model of coherent radiation interferometry. Based on the analysis of interferometer autocorrelation function (ACF), we can derive the information about temporal structure of the trains.

MODEL DESCRIPTION

In this section, we describe the mathematical model for the ACF simulation underlying the proposed approach. In general case, the intensity of radiation produced by the train registered by the detector after passing through the interferometer is determined by the following expressions:

$$I(\Delta l) = \int_{\nu_1}^{\nu_2} [N + N(N+1)F(\nu)] \frac{d^2W}{d\nu d\Omega} V(\nu)T(\nu)P(\nu)M(\nu)S(\nu),$$

$$F(\nu) = \frac{1}{m^2} e^{-\frac{4\pi^2\nu^2}{c^2}\left(\sigma_x^2 s_x^2 + \sigma_y^2 s_y^2 + \sigma_z^2 s_z^2\right)} \left| \sum_{j=1}^{m} e^{-i\frac{2\pi\nu}{c} l(j-1)s_z} \right|^2,$$

where ν is the radiation frequency, c is the speed of light in vacuum, $\{\nu_1, \nu_2\}$ is the detector sensitivity range, N is the electron number in the train, c is the speed of light, $\frac{d^2W}{d\nu d\Omega}$ is the spectral-angular distribution of radiation from one electron, $F(\nu)$ is the form-factor of a uniform electron bunch train, $S(\nu)$ is the detector sensitivity function, $M(\nu)$ is the interference multiplier, $T(\nu)$ is the multiplier responsible for transmission properties of the vacuum chamber window, $V(\nu)$ is the multiplier responsible for radiation propagation medium and splitter material in the interferometer, $P(\nu)$ is the multiplier responsible for the polarizer characteristics. In [2–4] you can find more information on how to calculate the bunch form-factor. As seen, the model takes into account the train structure parameters and the detector characteristics. The mechanisms of transition radiation (TR) and diffraction radiation (DR) are selected as the radiation source. Note that TR mechanism is invasive and DR one is noninvasive. The geometries of TR and DR generation are illustrated in Fig. 1. However, other type of radiation could be selected as a source (e.g., synchrotron or Cerenkov radiation).

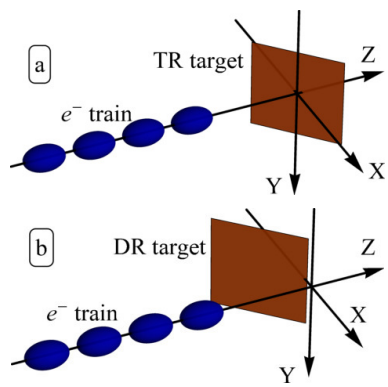

Figure 1: The schematic interaction geometries of the train with the target in cases of TR (a) and DR (b).

In these geometries, only the horizontal component of the radiation polarization is mainly present. It means that $\frac{d^2W}{d\nu d\Omega} \approx \frac{d^2W_z}{d\nu d\Omega}$.

SIMULATION

The simulation of the TR and DR spectra from single electron, illustrated in Fig. 2, was carried out based on the program written on the *Wolfram Language* code [5], developed earlier [6]. For numerical integration, the default method and the Monte Carlo method [7] was used[1]. In the simulation, the target is flat and has a finite size to be acceptable for use in the accelerator path. The θ_0 is the angle between the normal vector and the particle trajectory. The center of the TR target is located at the coordinate system center. The DR target edge is located at the distance equal to

* mmt8@tpu.ru
† shkitovda@tpu.ru

[1] {Automatic, "SymbolicProcessing"->False} and {"MonteCarlo", "MaxPoints"->10^8, Method->{"MonteCarloRule", "AxisSelector"->Random, "Points"->$5 * 10^6$}, "SymbolicProcessing"->False}

ISBN: 978-3-95450-240-0 ISSN: 2673-5539 doi:10.18429/JACoW-RuPAC2021-WEPSC36

the impact parameter from the system coordinate center. For a given value of the impact parameter (which $> 3\sigma$), we can speak of the non-perturbing nature of the interaction of the 0.1-mm transverse size bunch (or less) with the DR target. As the first step, the simulation was carried out for a simple case, the details of which are listed in Table 1. The simulation was conducted for the Michelson interferometer with interference multiplier equals to $M(\nu) = \left|1 + e^{-i2\pi\Delta l\nu/c}\right|^2$, where $\Delta l = 2d$ is the optical path difference and d is the interferometer movable mirror displacement. $M(\nu)$ is illustrated in Fig. 3. The $F(\nu)$ and $S(\nu)$ model components are presented in Fig. 4 with narrowband detector (ND) and broadband detector (BD). Note that the wide variety of THz detectors [8] are currently available.

Table 1: The Simulation Parameters

Target type	Perfect conductor
Target size	50 mm × 50 mm
Distance target center to detector, L	5 m
Impact parameter (for DR only), h	0.5 mm
Spectral frequency range simulation	0.01 –1.5 THz
Tilt angle of target (DR, TR), θ_0	45°, 46.5°
Energy of electrons, E_e	10 MeV
Longitudinal bunch size, σ_z	0.15 ps
Bunch transverse dimensions, σ_x, σ_y	0.1 mm
Charge distribution in the train	Uniform
Charge distribution of bunches	Gaussian
Number of bunches in the train, m	2–10
Train population, N	1000
Bunch spacing, l (BD, ND)	1 –7 ps, 9 –15 ps
BD sensitivity range	0.1 –1.4 THz
ND sensitivity range	0.5 –0.7 THz
$V(\nu)$, $T(\nu)$, $P(\nu)$	1

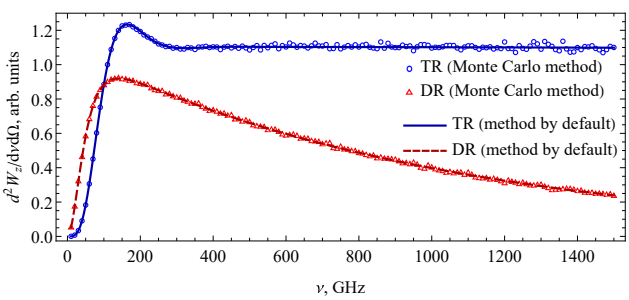

Figure 2: Spectral distributions of TR and DR.

RESULTS AND DISCUSSION

Simulation results for DR are presented in Fig. 5 and 6. Some outliers are due to numerical calculations. In general terms, the ACF represents the intensity dependence from Δl with the packet's set of oscillations. As can be seen, the packet's number connected the bunch number by the relation $m = (k + 1)/2$, where k is the number of oscillation packets in the ACF (see Fig. 5). There is the clear difference between

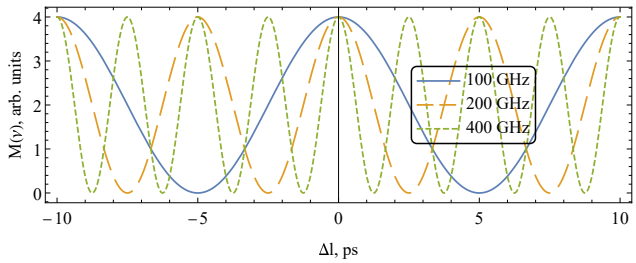

Figure 3: The examples of interference multiplier for different frequencies.

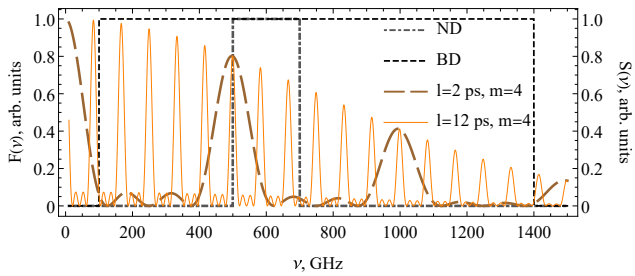

Figure 4: Form-factors of electron trains for two bunch spacing (both TR and DR cases are coincides) and detector sensitivity ranges for both ND and BD cases.

the ACF in case of ND and BD. With BD, we can distinguish the shorter bunch spacing in the train. It is important to have at least two peaks in the detector sensitivity range in order to get the clear packet structure. In Table 2 the comparison of l and estimated l_{est} is presented, where l_{est} is the average value of distance between peaks of ACF envelope curve (see Fig. 6). For TR case, the all findings will be the same.

Table 2: The Estimation of Spacing (in ps) for Fig. 6

ND	l	9	10	11	12	13	14	15
	l_{est}	8.7	10.6	10.8	12.3	12.8	14.4	14.7
BD	l	1	2	3	4	5	6	7
	l_{est}	1.0	2.0	3.0	4.0	5.0	6.0	7.0

CONCLUSION

We have demonstrated the technique for measuring the microbunches separation in a microbunch system by virtue of the coherent TR and DR autocorrelation function simulation. The obtained results are limited by the finite bandwidth of the detector. Thereby, the time delay between microbunches can be determined via measuring of autocorrelation curve employing a detector with an appropriate frequency range. The detection system with the broadband frequency response range allows for the measurement of a short time delay between microbunches. The technique proposed does not dependent on the microbunch train production method and is applicable to any number of microbunches. This technique shows that the usage of coherent diffraction radiation allows to control the time delay between microbunches without destruction of the electron beam.

ISBN: 978-3-95450-240-0 ISSN: 2673-5539 doi:10.18429/JACoW-RuPAC2021-WEPSC36

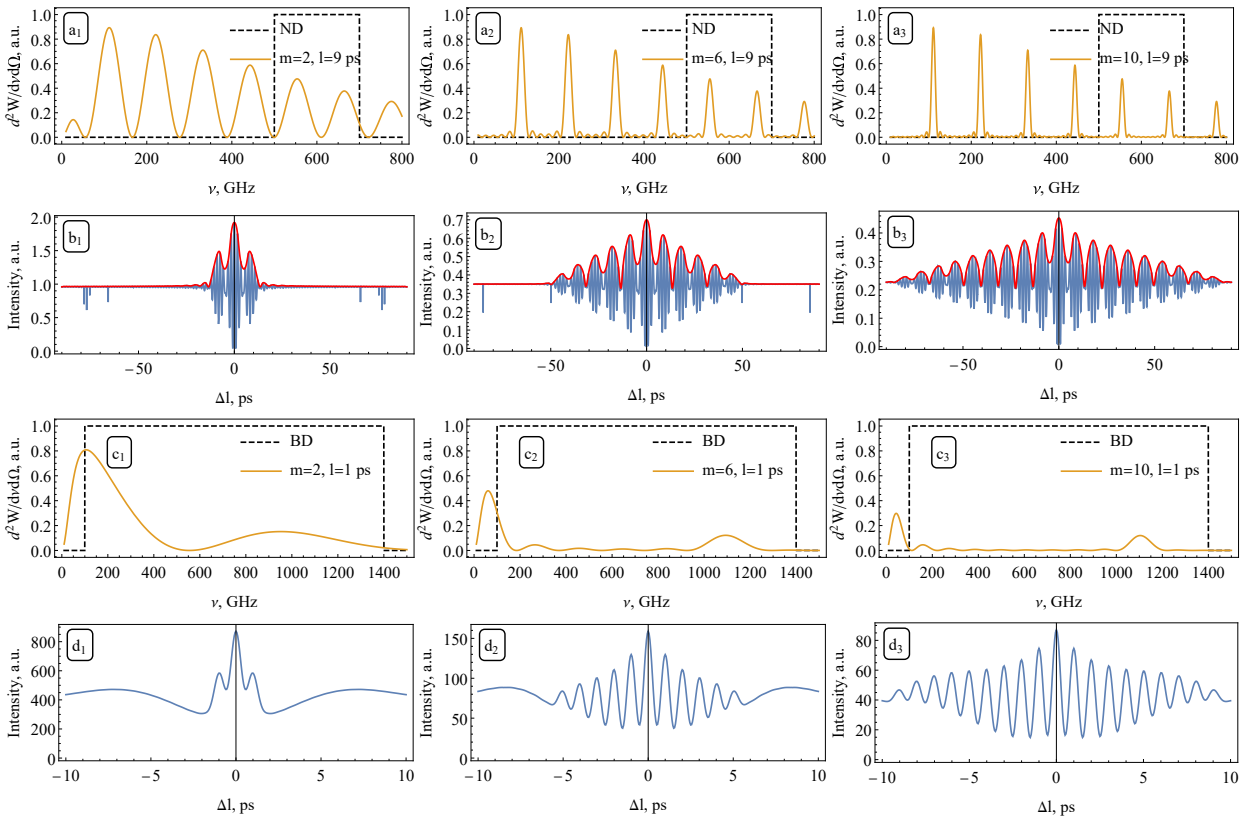

Figure 5: The DR spectra (a, c rows) and autocorrelation function (b, d rows) evolution in depends on increasing bunch number in train for both ND (a, b rows) and BD (c, d rows) case. The red line is the envelope curve.

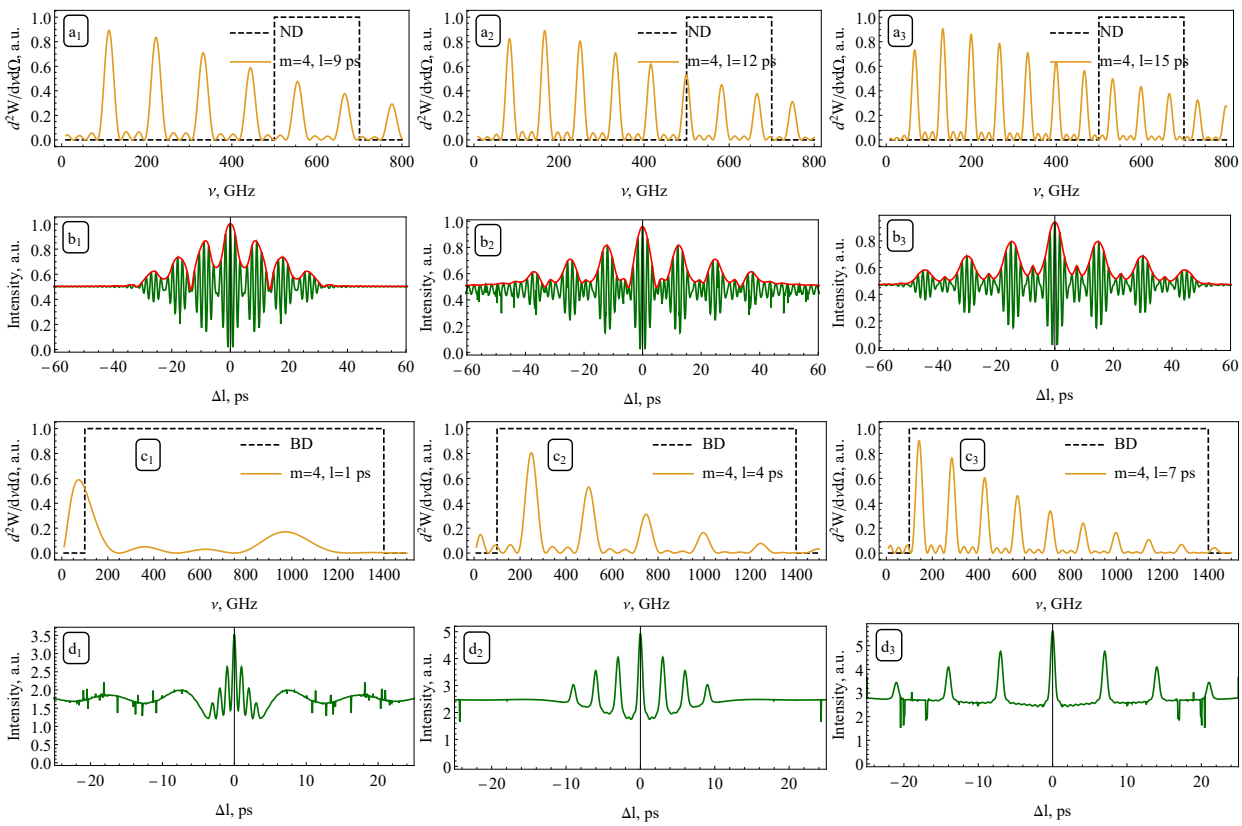

Figure 6: The same caption as on Fig. 5 but in depends on bunch spacing with fixed bunch number.

ISBN: 978-3-95450-240-0 ISSN: 2673-5539 doi:10.18429/JACoW-RuPAC2021-WEPSC36

REFERENCES

[1] S. Antipov *et al.*, "Subpicosecond bunch train production for a tunable mJ level THz source", *Phys. Rev. Lett.*, vol. 111, p. 134802, 2013. doi:10.1103/PhysRevLett.111.134802

[2] G. A. Naumenko, "Form-Factors of Relativistic Electron Bunches in Polarization Radiation", *Advanced Materials Research*, vol. 1084, p. 138, 2015. doi:10.4028/www.scientific.net/AMR.1084.138

[3] A. P. Potylitsyn, "Spatial coherence in transition radiation from short electron bunches", *JETP Lett.*, vol. 103, pp. 669–673, 2016. doi:10.1134/S0021364016110102

[4] Coherent Transition Radiation from Bunches of Charged Particles, https://demonstrations.wolfram.com

[5] Wolfram Language, https://www.wolfram.com/language

[6] D. A. Shkitov, "Code for simulation of diffraction radiation from flat finite surfaces", in *Proc. 26 th Russian Particle Accelerator Conf. (RuPAC'18)*, Protvino, Russia, Oct. 2018, pp. 510–513. doi:10.18429/JACoW-RUPAC2018-THPSC56

[7] NIntegrate Integration Rules, https://reference.wolfram.com/language/tutorial/NIntegrateIntegrationRules.html#430697921

[8] R. A. Lewis, "A review of terahertz detectors", *J. Phys. D: Appl. Phys.*, vol. 52, p. 433001, 2019. doi:10.1088/1361-6463/ab31d5